COMPARISON OF X-RAY LINE PROFILE AND DIP TEST MEASUREMENTS OF INTERNAL STRESSES DURING HIGH TEMPERATURE CREEP OF COPPER

KAREL MILIČKA[1], FERDINAND DOBEŠ*[1], ERHARD SCHAFLER[2], MICHAEL ZEHETBAUER[2]

Internal stresses resulting in polycrystalline copper from creep deformation at temperatures of 773 and 873 K were investigated by two different methods. The first one was the analysis of asymmetric X-ray line profiles. The second one was the dip test technique, which consisted in observation of strain rate after stress changes. The values of internal stresses obtained by these two methods turn out to be not identical, but a close analysis in terms of the composite model shows that the difference in data arises from differences in the definitions of internal stresses. A relation between the internal stresses based on the composite model has been derived which reveals that the data received by the two methods are fully compatible when a reasonable value of dislocation interaction coefficient is chosen.

K e y w o r d s: creep, internal stress, X-ray diffraction profiles, dip test, composite model

POROVNÁNÍ VNITŘNÍCH NAPĚTÍ PŘI VYSOKOTEPLOTNÍM CREEPU MĚDI MĚŘENÝCH RENTGENOGRAFICKY A TECHNIKOU ZMĚN NAPĚTÍ

Vnitřní napětí vznikající při creepové deformaci mědi při teplotách 773 a 873 K byla studována dvěma technikami. První z nich byla analýza asymetrických profilů rentgenových difrakčních čar. Druhá technika využívala metodu „dip testu“, která spočívala ve stanovení zbytkového aplikovaného napětí, po kterém je pozorována nulová rychlost deformace. Hodnoty vnitřního napětí získané těmito dvěma metodami nejsou identické. Detailnější analýza pomocí kompozitního modelu ukazuje, že rozdíly v měřených hodnotách jsou způsobeny odlišnými definicemi vnitřních napětí. Je odvozen vztah mezi vnitřními

[1] Institute of Physics of Materials, Academy of Sciences of the Czech Republic, Žižkova 22, 616 62 Brno, Czech Republic
[2] Institute of Materials Physics, University of Vienna, Strudlhofgasse 4, A-1090 Wien, Austria
* corresponding author, e-mail: dobes@ipm.cz

napětími založený na kompozitním modelu, který dokládá, že údaje získané dvěma metodami jsou plně kompatibilní, pokud se zvolí vhodná hodnota dislokačního interakčního koeficientu.

1. Introduction

A general feature of microstructures in single-phase materials deformed at both room temperature and at elevated temperatures is the existence of heterogeneous distribution of dislocations. Regions of tangles, cell walls or subgrain boundaries with high dislocation density separate the regions of lower dislocation density in cells or in subgrain interiors [1]. The occurrence of heterogeneous microstructure is accompanied by long-range internal stresses. This was first proved by the observation of curved dislocation segments in the vicinity of subgrain boundaries [2]. The subsequent high-resolution X-ray diffraction experiments enabled the quantitative evaluation of such internal stresses by an analysis of asymmetry of X-ray line profiles [3]. The positive (i.e. forward) internal stresses are observed in cell walls/subgrain boundaries areas, $\Delta\sigma_{\mathrm{w}}$, and these are compensated by negative (i.e. backward) internal stresses in cell/subgrain interiors, $\Delta\sigma_{\mathrm{c}}$. By the X-ray method applied in the present article, the difference of the above local internal stresses is determined, $|\Delta\sigma_{\mathrm{w}} - \Delta\sigma_{\mathrm{c}}|$. In what follows, this quantity will be designated as the *long-range internal stress*.

The stress acting on a moving dislocation can be divided into (i) a component that overcomes the stresses generated by neighbouring dislocations or other long--range obstacles and (ii) a component that opposes a velocity-dependent lattice friction. This idea was a motivation to apply another method for estimation of internal stresses, known as the dip test technique [4]. The method consists in a reduction of the applied stress to the level, at which the strain rate equals zero. The internal stress is then defined as the residual stress acting on the specimen after the critical stress change, $\sigma_{\mathrm{i}} = \sigma - \Delta\sigma_{\mathrm{crit}}$. We will designate this quantity as the *dip-test internal stress*.

In the present contribution, the results of measurements carried out by both methods on identical polycrystalline Cu samples, which have been deformed by creep at high deformation temperatures, are presented. The paper also reports on quantitative relations between the long-range internal stress, $|\Delta\sigma_{\mathrm{w}} - \Delta\sigma_{\mathrm{c}}|$, as measured by the X-ray line profile analyses and the dip-test internal stress, σ_{i}, by performing stress dip tests.

2. Experimental technique

2.1 Creep tests and dip test measurement

For the experiments, oxygen-free copper of purity higher than 99.99 % was used. Specimens had a gauge length 12 mm and a cross section diameter 6 mm.

The average grain size was 0.10 mm. The creep tests were performed in argon atmosphere under constant compressive stress at temperatures of 773 and 873 K, respectively. The stress was maintained constant by means of a modified lever system [5]. Creep deformation was measured using the linear variable differential transducer (W2K or W5K by Hottinger-Baldwin Co.), and was continuously PC-recorded. The recording frequency of the transient strain response after stress change was 12 Hz. The internal stress in steady state creep was measured by the strain transient dip test technique proposed by Ahlquist and Nix [4]. Stress changes were performed in steady-state stage only. Time spent at reduced stress was limited to a minimum necessary for a safe determination of the creep rate after the stress reduction (typically less than 10 sec). After this time, the specimen was reloaded to the original stress value. It was possible to perform about 10 of such stress reductions in period of the steady state creep in one test. Sufficient strain was left between subsequent stress reductions, so that the creep rate could recover to its original steady-state level. The specimens for X-ray measurements were crept at the same conditions as in the dip tests, but without stress changes.

2.2 X-ray Bragg peak profile analysis (XPA)

The 0.3×3 mm line focus of an AXS Bruker rotating Cu anode was used, operating at 45 kV and up to 100 mA. The primary X-ray beam was monochromatized by an asymmetrically cut plane Ge crystal using the 444 reflection and tuned to CuKα_1 line ($l = 1.54$ Å). The cross section of the footprint of the beam on the sample was about 0.1×1 mm^2. The scattered radiation was registered by a linear position sensitive X-ray detector type OED-50 (Braun, Munich, FRG). The sample-to-detector distance was about 1 m. The {200} reflection was measured.

2.3 Evaluation of X-ray diffraction profiles

The determination of the dislocation densities and long-range internal stresses has been carried out from single Bragg reflection profiles [3]. In the case of large crystals containing dislocations, the real part of the Fourier coefficients of a profile can be written as:

$$\ln|A(n)| = -\rho^* n^2 \ln\left(\frac{R_\mathrm{e}}{n}\right) + Q^* n^4 \ln\left(\frac{R_2}{n}\right) \ln\left(\frac{R_3}{n}\right) \pm \mathrm{O}(n^6), \qquad (1)$$

where ρ^* is the "formal" dislocation density, directly available from a broadened profile without taking into account the different types of dislocations and the relative orientation of their Burgers and line vector to the diffraction vectors. Q^*, in the simplest case, can be interpreted as the spatial fluctuation of the dislocation density, R_e is the outer cut-off radius of dislocations, R_2 and R_3 are auxiliary constants and n is the Fourier parameter [6]. Terms of the order of 6 and higher can be

neglected [7]. For the present measurements, spatial fluctuations of dislocation density are not considered because their magnitude is below the measuring accuracy. Thus, the true dislocation density ρ can be calculated from the formal (measured) one ρ^* [6–8], by the relation

$$\rho = \rho^* \frac{2}{\pi \boldsymbol{g}^2 \boldsymbol{b}^2 \bar{C}}, \tag{2}$$

where $\bar{C}$ is the average contrast factor, $\boldsymbol{g}$ the diffraction vector and $\boldsymbol{b}$ the Burgers vector of dislocations. $\bar{C}$ can be calculated numerically on the basis of the crystallography of dislocations and from the elastic constants of a crystal [8, 9]. In the present work, samples were measured in axial case ($\boldsymbol{g}$ being parallel to deformation axis). Following the procedure described in [10] and considering {110} Burgers vectors to be activated during compression on both faces 2 and 3 of the cubic elementary cell (for definition see [10]), $\bar{C} = 0.306$ results, assuming screw and edge dislocations to be generated to equal parts. Together with known data for $\boldsymbol{g}$ and $\boldsymbol{b}$ and the measured dislocation density ρ^*, the true dislocation density ρ can be now calculated by means of Eq. (2).

The long range internal stresses arise from the fact that with progressing plastic deformation the dislocations arrange in hard "cell walls" and soft "cell interiors", where the cell walls contain a high dislocation density compared to a much lower one in the cell interior regions. This leads to different stress levels $\Delta\sigma_\mathrm{w}$ and $\Delta\sigma_\mathrm{c}$ weighted by their volume fraction, which, considering the "composite model" of Mughrabi and co-workers, have to be in balance [3, 11]. The result for the X-ray line profile is an asymmetry arising from the composition of two sub-profiles corresponding to differently strained cell-wall and cell-interior regions shifted differently from the center of gravity of the measured profile. Using Hooke's law, the local internal stresses $\Delta\sigma_\mathrm{w}$ and $\Delta\sigma_\mathrm{c}$ can be calculated from the individual shifts of the sub-profiles, which lead to the long range internal stresses $|\Delta\sigma_\mathrm{w} - \Delta\sigma_\mathrm{c}|$ between the areas of cell walls and cell interiors [3, 10]. The volume fraction of hard regions f_w and that of soft regions $(1 - f_\mathrm{w})$ are determined from the proportion of the integral intensities of respective sub-profiles.

3. Experimental results

The results of measurements of the internal stresses are presented in Fig. 1. The dip-test internal stress σ_i is increasing with increasing applied stress. The dependence is similar to that observed in many pure metals and solid solutions – a review can be found in Ref. [12]. On the other hand, no such dependence can be seen in the behaviour of the long-range internal stress $|\Delta\sigma_\mathrm{w} - \Delta\sigma_\mathrm{c}|$. The dislocation density estimated from the X-ray measurements is presented in Fig. 2. The dislocation density is approximately proportional to the square of the applied

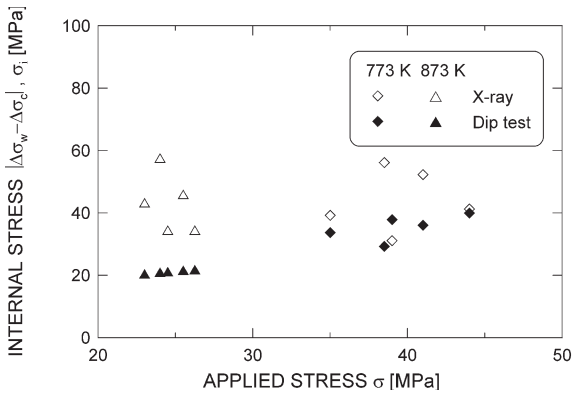

Fig. 1. Applied stress dependence of the internal stress measured by two techniques.

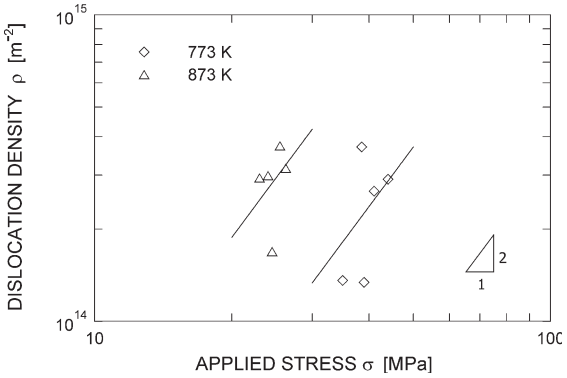

Fig. 2. Applied stress dependence of the total dislocation density measured by X-ray technique.

stress, which is in accordance with the Taylor's formula

$$\sigma \propto Gb\sqrt{\rho}, \tag{3}$$

where G is the shear modulus and b is the Burgers vector length. The temperature dependence of the dislocation density is clearly stronger than that of the shear modulus. The volume fractions of the subgrain wall areas derived from X-ray diffraction measurements are presented in Fig. 3.

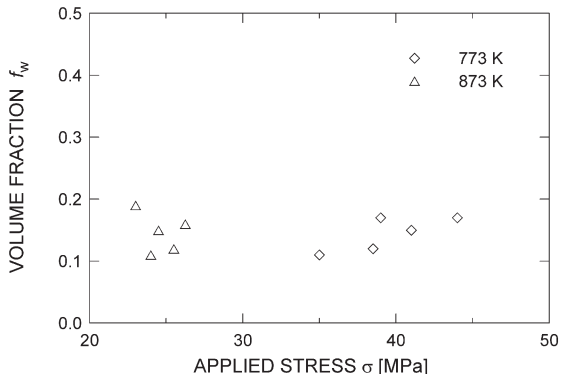

Fig. 3. Applied stress dependence of the volume fraction of hard regions.

4. Discussion

As it was stated above, the applied stress in heterogeneous structures is redistributed to σ_w in hard regions (cell or subgrain boundaries, respectively) and σ_c in soft regions (cell/subgrain interiors). The stresses must fulfill the condition of mechanical equilibrium

$$\sigma = f_\mathrm{w}\sigma_\mathrm{w} + (1 - f_\mathrm{w})\sigma_\mathrm{c}. \tag{4}$$

Both the local stresses can be divided into the component overcoming the local long-range internal stresses and the component opposing a velocity-dependent internal friction:

$$\sigma_\mathrm{w} = \sigma_\mathrm{iw} + \sigma_\mathrm{w}^*, \tag{5a}$$

$$\sigma_\mathrm{c} = \sigma_\mathrm{ic} + \sigma_\mathrm{c}^*. \tag{5b}$$

In the model described by Mughrabi [13] or by Sedláček [14], the moving dislocation extends over both hard and soft regions and the density of moving dislocations, ρ_m, is the same in both regions. Due to the compatibility condition, the strain rate is also the same in both regions and the dislocation velocities equal each other. The local dislocation velocities are then given by [15]

$$v_\mathrm{w} = v_0 \sinh\left(\frac{A_\mathrm{w} b\sigma_\mathrm{w}^*}{MkT}\right), \tag{6a}$$

$$v_\mathrm{c} = v_0 \sinh\left(\frac{A_\mathrm{c} b\sigma_\mathrm{c}^*}{MkT}\right), \tag{6b}$$

where v_0 is a temperature dependent (and structure independent) term, A_w and A_c are respective activation areas, M is the Taylor factor (in polycrystalline copper $M = 3.06$), k is the Boltzmann constant and T is the absolute temperature. The activation area equals to the product of activation length and the length of the Burgers vector b. In pure metals, the activation length is proportional to the dislocation distance [16] and thus

$$A_\mathrm{w} = \frac{\omega_\mathrm{w} b}{\sqrt{\rho_\mathrm{w}}}, \tag{7a}$$

$$A_\mathrm{c} = \frac{\omega_\mathrm{c} b}{\sqrt{\rho_\mathrm{c}}}, \tag{7b}$$

where ρ_w and ρ_c are local dislocation densities in hard and in soft regions, and ω_w and ω_c are respective proportionality constants. These constants are probably different in different types of dislocation structures in subgrain boundaries and in subgrain interiors. For the sake of simplicity, we will put in the following numerical calculations $\omega_\mathrm{w} = \omega_\mathrm{c} = \sqrt{3}$, which corresponds to regular three-dimensional dislocation network. The local effective stress is given as a difference of the local applied stress and the local internal stress from neighbouring dislocations

$$\sigma_\mathrm{w}^* = \sigma_\mathrm{w} - \alpha M G b \sqrt{\rho_\mathrm{w}}, \tag{8a}$$

$$\sigma_\mathrm{c}^* = \sigma_\mathrm{c} - \alpha M G b \sqrt{\rho_\mathrm{c}} \tag{8b}$$

provided that the dislocation interaction coefficient α is the same for dislocations in cell walls and cell interior. It follows from the above stated equality of dislocation velocities in hard and soft regions, and by making use of Eqs. (6, 7, 8) that

$$\frac{\sigma_\mathrm{w}}{\sqrt{\rho_\mathrm{w}}} = \frac{\sigma_\mathrm{c}}{\sqrt{\rho_\mathrm{c}}} \ . \tag{9}$$

After a stress change, the local stress values in the hard and soft regions adjust to the new values corresponding to changed external conditions. The total strain rate as registered immediately after the stress change is thus given by the sum of elastic and plastic components. For the critical stress reduction in dip test, the total strain rate equals zero:

$$\frac{\dot\sigma_\mathrm{w}}{E} + \frac{\rho_\mathrm{m} b v_0}{M} \sinh\left[\frac{\sqrt{3} b^2 (\sigma_\mathrm{w} - \Delta\sigma_\mathrm{crit} - \alpha M G b \sqrt{\rho_\mathrm{w}})}{M k T \sqrt{\rho_\mathrm{w}}}\right] = 0, \tag{10a}$$

$$\frac{\dot\sigma_\mathrm{c}}{E} + \frac{\rho_\mathrm{m} b v_0}{M} \sinh\left[\frac{\sqrt{3} b^2 (\sigma_\mathrm{c} - \Delta\sigma_\mathrm{crit} - \alpha M G b \sqrt{\rho_\mathrm{c}})}{M k T \sqrt{\rho_\mathrm{c}}}\right] = 0. \tag{10b}$$

For the plastic strain rate, the relation $\mathrm{d}\varepsilon/\mathrm{d}t = \rho_\mathrm{m} b v/M$ has been used here, where v was taken from (6).

If the time derivative of the volume fractions f_w and f_c can be neglected (and this assumption is quite plausible since the applied stress dependence of the volume fractions is negligible and, moreover, it is assumed that the structure does not change in dip tests experiments), it follows from the Eq. (4) that in creep conditions

$$f_\mathrm{w}\dot{\sigma}_\mathrm{w} + f_\mathrm{c}\dot{\sigma}_\mathrm{c} = 0. \tag{11}$$

From Eqs. (10) and (11) we get

$$\begin{aligned} f_\mathrm{w} \sinh\left[\frac{\sqrt{3}b^2(\sigma_\mathrm{w} - \Delta\sigma_\mathrm{crit} - \alpha MGb\sqrt{\rho_\mathrm{w}})}{MkT\sqrt{\rho_\mathrm{w}}}\right] + \\ + f_\mathrm{c} \sinh\left[\frac{\sqrt{3}b^2(\sigma_\mathrm{c} - \Delta\sigma_\mathrm{crit} - \alpha MGb\sqrt{\rho_\mathrm{c}})}{MkT\sqrt{\rho_\mathrm{c}}}\right] = 0. \end{aligned} \tag{12}$$

Equation (12) can be solved numerically for $\Delta\sigma_\mathrm{crit}$ and thus the dip test internal stress can be calculated from the X-ray data, as will be shown as follows: Analytical solutions can be given for particular values of different arguments in the sinh function:

small arguments:

$$\sigma_\mathrm{i} = \sigma - \frac{\sigma_\mathrm{c} - \alpha MGb\sqrt{\rho_\mathrm{c}}}{f_\mathrm{c} + f_\mathrm{w}\dfrac{\sigma_\mathrm{c}}{\sigma_\mathrm{w}}}; \tag{13}$$

large arguments:

$$\sigma_\mathrm{i} = \sigma - \frac{2\,(\sigma_\mathrm{c} - \alpha MGb\sqrt{\rho_\mathrm{c}}) - \dfrac{MkT}{b^2}\ln\left(\dfrac{f_\mathrm{c}}{f_\mathrm{w}}\right)\sqrt{\dfrac{\rho_\mathrm{c}}{3}}}{1 + \dfrac{\sigma_\mathrm{c}}{\sigma_\mathrm{w}}}. \tag{14}$$

By convincing oneself that the quantities σ_c, σ_w, f_c, and f_w are accessible by the X-ray diffraction experiments (see footnote*), it comes evident that the internal

* The simultaneous measurement of the volume fraction f_w and the long-range internal stress $\Delta\sigma_\mathrm{w} - \Delta\sigma_\mathrm{c}$ by the X-ray technique offers possibility to calculate the local stresses in the hard and soft regions:

$$\sigma_\mathrm{w} = \sigma + (1 - f_\mathrm{w})(\Delta\sigma_\mathrm{w} - \Delta\sigma_\mathrm{c}), \tag{15a}$$

$$\sigma_\mathrm{c} = \sigma - f_\mathrm{w}(\Delta\sigma_\mathrm{w} - \Delta\sigma_\mathrm{c}). \tag{15b}$$

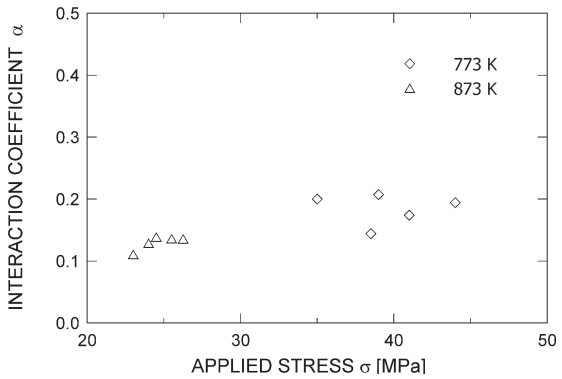

Fig. 4. Calculated values of the dislocation interaction coefficient in dependence on applied stress.

stresses measured by different techniques are neither identical nor that their relation is straightforward. The results of calculation of dip-test internal stresses via Eqs. (12), (13) or (14) are sensitive to the value of interaction coefficient α. Values of α calculated from Eq. (12) that lead to full compatibility of the dip-test internal stress and of the X-ray measurements are given in Fig. 4. They all amount to about 0.1 that is in agreement with an analysis done by Lavrentev [17].

5. Comparison of measured internal stress data with available literature

The local stresses can be expressed in terms of the stress intensity factors, e.g., $k_\mathrm{w} = \sigma_\mathrm{w}/\sigma$. A comparison of this quantity with the relevant data reported previously by Straub et al. [18] for copper crept at temperatures ranging from 298 to 633 K at constant normalized stress $\sigma/G = 0.0043$ is given in Figs. 5 and 6. The results confirm the conclusion suggested by Straub et al. [18] that the stress concentration factor increases with increasing deformation temperature.

Dislocation densities in cell/subgrain boundaries, ρ_w, and in cell/subgrain interiors, ρ_c, are coupled by the relation [19]

$$\rho = f_\mathrm{w}\rho_\mathrm{w} + f_\mathrm{c}\rho_\mathrm{c}. \tag{16}$$

Owing to Eq. (9), both dislocation densities can be calculated from the data received from X-ray measurements

$$\rho_\mathrm{w} = \frac{\rho}{f_\mathrm{w} + f_\mathrm{c}\left(\sigma_\mathrm{c}/\sigma_\mathrm{w}\right)^2}, \tag{17a}$$

$$\rho_\mathrm{c} = \frac{\rho}{f_\mathrm{c} + f_\mathrm{w}\left(\sigma_\mathrm{w}/\sigma_\mathrm{c}\right)^2}. \tag{17b}$$

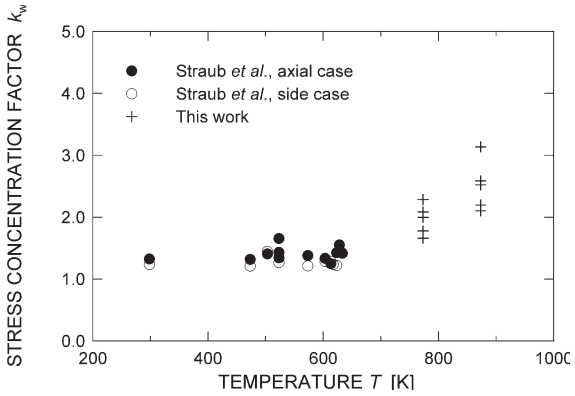

Fig. 5. Temperature dependence of the stress concentration factor. Comparison with the results of Straub et al. [18].

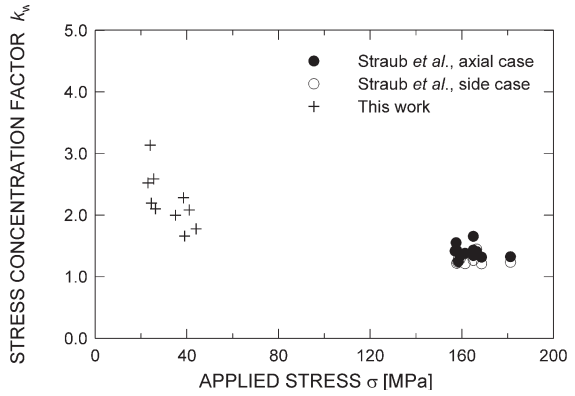

Fig. 6. Applied stress dependence of the stress concentration factor. Comparison with the results of Straub et al. [18].

The dislocation density in subgrain interiors calculated by means of Eq. (17b) can be compared with the data obtained by transmission electron microscopy. A review of existing data in copper was published by Mughrabi [20]. The comparison is illustrated in Fig. 7 in terms of the normalized dislocation distance in subgrain interiors $l_c/b = \sqrt{3/\rho_c}/b$.

A comparison of the volume fraction of hard regions obtained in the present work with the data published previously by Straub et al. [18] is given in Fig. 8. The plot clearly demonstrates a relatively great scatter of this measurement. The present data show that the tendency of f_w to decrease with increasing temperature,

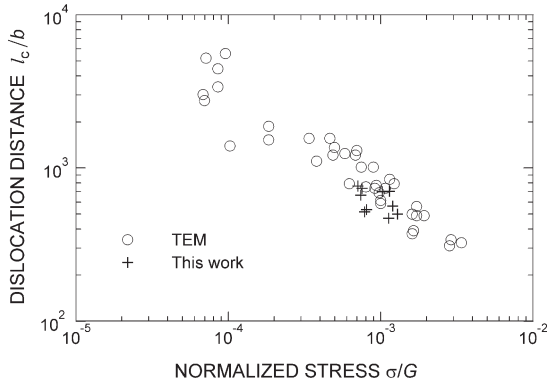

Fig. 7. Comparison of the calculated normalized dislocation distance with the same distance measured by transmission electron microscopy as reviewed by Mughrabi [20].

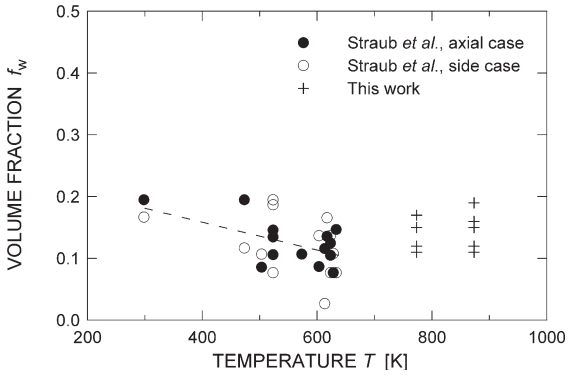

Fig. 8. Temperature dependence of the volume fraction of hard regions. Comparison with the data of Straub et al. [18].

which was ascribed to the transition from cell to subgrain structure [18] is not continued at deformation temperatures $T > 0.5\,T_{\mathrm{M}}$, where T_{M} is the absolute melting temperature.

6. Conclusions

1. The long-range internal stress derived from X-ray measurements corresponds to the amplitude of local internal stresses, while the internal stress evaluated from the dip-test does not. A quantitative method for comparison of both internal stresses is presented.

2. Full compatibility of the presented values of the dip-test internal stress and the X-ray long-range internal stress can be achieved when realistic values of the dislocation interaction coefficient are used.

3. The mean distance of dislocations in subgrain interiors calculated from the local internal stress is in agreement with the values found by transmission electron microscopy investigations.

Acknowledgements

The investigation was performed within the frame of a Joint Austrian – Czech project granted by the Österreichisches Ost- und Südosteuropa Institut. A partial support of the Grant Agency of the Academy of Sciences of the Czech Republic within the grant A2041202 is gratefully acknowledged. M. Z. and E. S. are grateful to the Austrian Science Foundation (FWF) that provided finances within project P12945.

REFERENCES

[1] HANSEN, N.—HUANG, X.—HUGHES, D. A.: Mater. Sci. Engng., *A317*, 2001, p. 3.
[2] CAILLARD, D.—MARTIN, J. L.: Acta Metall., *30*, 1982, p. 791.
[3] UNGÁR, T.—MUGHRABI, H.—RÖNNPAGEL, D.—WILKENS, M.: Acta Metall., *32*, 1984, p. 333.
[4] AHLQUIST, C. N.—NIX, W. D.: Scripta Metall., *3*, 1969, p. 679.
[5] DOBEŠ, F.—ZVEŘINA, O.—ČADEK, J.: J. Test. Eval., *14*, 1986, p. 271.
[6] UNGÁR, T.—GROMA, I.—WILKENS, M.: J. Appl. Cryst., *22*, 1989, p. 26.
[7] GROMA, I.—UNGÁR, T.—WILKENS, M.: J. Appl. Cryst., *21*, 1988, p. 47.
[8] WILKENS, M.: Phys. Stat. Sol. (a), *2*, 1970, p. 359.
[9] WILKENS, M.: Phys. Stat. Sol. (a), *104*, 1987, p. K1.
[10] MÜLLER, M.—ZEHETBAUER, M.—BORBÉLY, A.—UNGÁR, T.: Z. Metallkde., *86*, 1995, p. 827.
[11] MUGHRABI, H.: Acta Metall., *31*, 1983, p. 1367.
[12] TAKEUCHI, S.—ARGON, A. S.: J. Mater. Sci., *11*, 1976, p. 1542.
[13] MUGHRABI, H.: Phys. Stat. Sol. (a), *104*, 1987, p. 107.
[14] SEDLÁČEK, R.: Scripta Metall. Mater., *33*, 1995, p. 283.
[15] LI, J. C. M.: In: Dislocation Dynamics. Eds.: Rosenfield, A. R., Hahan, G. T., Bement, A. L., Jaffee, R. I. New York, McGraw-Hill 1968, p. 87.
[16] SEEGER, A.: Encyclopaedia of Physics. Vol. 7/2. Berlin, Springer Verlag 1958.
[17] LAVRENTEV, F. F.: Mater. Sci. Engng., *46*, 1980, p. 191.
[18] STRAUB, S.—BLUM, W.—MAIER, H. J.—UNGÁR, T.—BORBÉLY, A.—RENNER, H.: Acta Mater., *44*, 1996, p. 4337.
[19] MUGHRABI, H.: Mater. Sci. Engng., *A85*, 1987, p. 15.
[20] MUGHRABI, H.: In: Constitutive Equations in Plasticity. Ed.: Argon, A. S. Cambridge, Mass., MIT Press 1975, p. 199.

Received: 25.11.2002
Revised: 30.1.2003